

Photometry of the 1991 Superoutburst of EF Pegasi: Super-Quasi-Periodic Oscillations with Rapidly Decaying Periods

Taichi KATO

Department of Astronomy, Kyoto University,
Sakyo-ku, Kyoto 606-8502

tkato@kusastro.kyoto-u.ac.jp

Abstract

We observed the 1991 October outburst of EF Peg. Prominent superhumps with a period of 0.08705(1) d were observed, qualifying EF Peg as a being long-period SU UMa-type dwarf nova. The superhump period showed a monotonous decrease during the superoutburst, which makes a contrast to the virtually zero period change observed during the 1997 superoutburst of the same object. Large-amplitude, and highly coherent quasi-periodic oscillations (super-QPOs) were observed on October 18, when superhumps were still growing in amplitude. Most strikingly, the QPOs showed a rapid decrease of the period from 18 m to 6.8 m within the 3.2-hr observing run. Such a rapid change in the period has not been observed in any class of QPOs in cataclysmic variables. We propose a hypothesis that the rapid decrease of the QPO period reflects the rapid removal of the angular momentum from an orbiting blob in the accretion disk, via the viscosity in a turbulent disk. A brief comparison is given with the QPOs in X-ray binaries, some of which are known to show a similar rapid decrease in the periods.

Key words: accretion, accretion disks — stars: novae, cataclysmic variables — stars: dwarf novae — stars: individual (EF Pegasi)

1 Introduction

1.1 Quasi-periodic oscillations

Quasi-periodic oscillations (QPOs) are short-period, quasi-periodic oscillations widely observed in accreting binary systems, such as cataclysmic variables (CVs) and X-ray binaries (XBs; see van der Klis (1989); more recent reviews particularly stressing on “kilohertz QPOs” include van der Klis (1999, 2000). There are two major types of “quasi-periodic” oscillations in CVs: dwarf nova oscillations (DNOs) and (in a narrower sense) QPOs (for a review, see Warner 1995a).

DNOs are oscillations observed only in dwarf nova outbursts, having periods 19–29 s, and have long (several tens to ~ 100 wave numbers) coherence times (Robinson (1973); Szkody (1976); Patterson (1981);

Hildebrand et al. (1980)). The amplitudes of DNOs in optical wavelengths are generally small (usually < 0.01 mag). Several models have been proposed to account for DNOs (and QPOs in general), including vertical or radial oscillations of the accretion disk (Kato, 1978), reprocessing of the light by the orbiting blobs (Patterson, 1979), non-radial pulsations of the accretion disk (Papaloizou, Pringle (1978); van Horn, Wesemael (1980)), radial oscillation of the accretion disk (Cox (1981); Blumenthal et al. (1984); Okuda, Mineshige (1991); Okuda et al. (1992)), excitation of trapped oscillations around the discontinuity of physical parameters (Yamasaki et al., 1995), and oscillation of the boundary layer of the accretion disk (Collins et al. 1998, 2000aa,b).

QPOs (other than DNOs¹) are more widely seen in CVs, having periods 40 s to several hundred seconds, have much shorter (usually less than ~ 10 wave numbers) coherence lengths. These less coherent QPOs have phenomenological similarities with QPOs in XBs, both in their coherence lengths and in the characteristic periods scaled by the Keplerian timescales at the inner edge of the accretion disk.

A potentially new class of QPOs (super-QPOs) were discovered during the 1992 superoutburst of SW UMa (Kato et al., 1992). These QPOs were only observed during the particular stages (usually the initial stage) of superoutbursts (for a review of SU UMa-type dwarf novae and superoutbursts, see Warner 1995b), and have periods of several hundred seconds, comparable to those of QPOs other than DNOs. The most striking features of super-QPOs were the large amplitudes (up to 0.2 mag) and the long coherence, lasting at least several tens of wave numbers (Kato et al., 1992). The super-QPOs observed by Kato et al. (1992) consisted of sinusoidal components and short, deep dips. Kato et al. (1992) also suggested that the QPOs reported by Robinson et al. (1987) showed only the sinusoidal components, but sharing all the other characteristics with super-QPOs observed during the 1992 superoutburst. Kato et al. (1992) proposed that an orbiting blob, which incidentally eclipsed the central part of the accretion disk, was responsible for the large-amplitude super-QPOs. Kato et al. (1992) suggested that the reason why super-QPOs are only observed during the particular stage of superoutburst may be that such a blob can be formed under the enhanced dissipation (i.e. turbulent condition) caused by the tidal instability, which is responsible for superhumps (Whitehurst (1988); Hirose, Osaki (1990)). Studies of super-QPOs have been, however, hindered by the paucity of examples. EF Peg is the only other example, which showed the remarkable time evolution of super-QPOs during the 1991 super-

¹We use the term “QPOs” in this sense in the rest of this paper.

outburst.

1.2 EF Peg

EF Peg was originally discovered as a variable star (Hoffmeister, 1935), who suggested the Mira-type classification. Esch (1937) recorded two additional (bright and faint ones) maxima, and derived a period of 157 d in combination with the maxima recorded by Hoffmeister (1935). However, Sandig (1950) only recorded an apparently nonvariable star of 13.5–14.0 photographic magnitude on 157 plates. Tsesevich et al. (1979) finally revealed that the true EF Peg is a normally fainter companion to a nonvariable star (labeled as *w* in Tsesevich et al. (1979) and Howell et al. (1993)). Tsesevich et al. (1979) suggested that EF Peg is a dwarf nova with a large outburst amplitude. Their observations showed the existence of two types of — short and long — outbursts, which strongly suggested an SU UMa-type dwarf nova (for a recent review of SU UMa-type stars and their observational properties, see Warner (1995b)). Upon this information, the Variable Star Observers League in Japan (VSOLJ) called for a monitoring campaign for an outburst since 1985. Gessner (1988) searched Sonneberg plates, and found nine outbursts between 1928 and 1986, confirming the classification by Tsesevich et al. (1979). No firm outbursts above a magnitude of 12 had been recorded until the discovery of an outburst by Patrick Schmeer on 1991 October 15.779 UT at visual magnitude 10.9 (Schmeer, Poyner, 1991). Since then, only two secure outbursts have been observed in 1995 January and 1997 October, according to the reports to the VSNET Collaboration², and no further outburst has been observed up to 2001 July. These observations indicate the intrinsically low outburst frequency of this object. Politano et al. (1998) even suggested that EF Peg is past the period minimum of the CV evolution. The first detection of superhumps was made by Kato, Takata (1991) on 1991 October 18. More information of this superoutburst is given in Howell et al. (1993).

2 Observations

The observations were performed with the CCD camera (Thomson TH7882 chip, 576×384 pixels) attached to the 0.6-m reflector at Ouda Station, Kyoto University (Ohtani et al., 1992) for seven nights between 1991 October 18 and 25. An on-chip summation of 3×3 pixels was adopted to minimize the readout time and noise. A Johnson *V*-band filter was adopted. The exposure time was generally 10 s, except on October 25, when the exposure time of 20 s was used. The readout time between

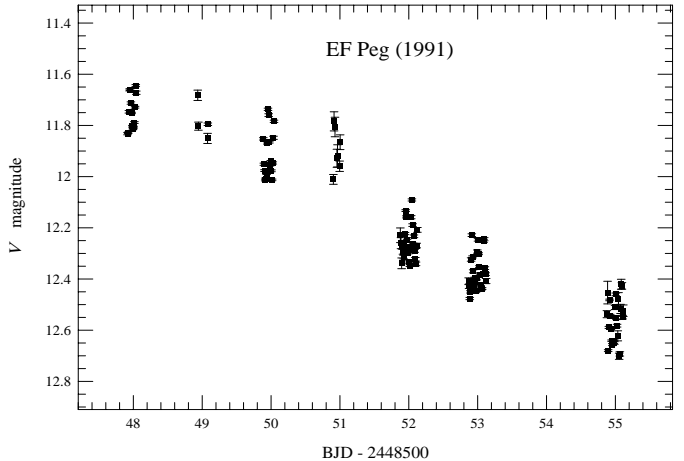


Figure 1: Overall behavior of the 1991 superoutburst of EF Peg, constructed from the CCD observations at Ouda. Each point and error bar represent an average and the standard error of the average of observations in each 0.01 d bin. A constant contribution from the $V=12.71$ companion star has been subtracted.

Table 1: Log of observations.

UT (start–end)	N*	mag [†]	error [‡]	exp
1991 October				
18.408 – 18.542	642	1.161	0.002	10
19.429 – 19.581	113	1.178	0.010	10
20.381 – 20.543	793	1.277	0.002	10
21.386 – 21.551	191	1.256	0.012	10
22.373 – 22.627	1161	1.494	0.002	10
23.366 – 23.625	1148	1.562	0.002	10
25.373 – 25.619	741	1.673	0.003	20

*Number of frames.

[†]Magnitude relative to BD +14°4648;

combined magnitude with the close companion.

[‡]Standard error of averaged magnitude.

^{||}Exposure time (s).

² (<http://www.kusastro.kyoto-u.ac.jp/vsnet/>)

exposures was 7–9 s. The total number of useful frames was 4789.

A summary of observation is listed in table 1. The CCD frames were, after standard de-biasing and flat-fielding, analyzed using automatic microcomputer-based aperture photometry package developed by the author. The diameter of the aperture was 18". The magnitudes of the object were determined relatively using a local standard star BD +14°4648 = GSC 1117.2097 (star *a* in Howell et al. (1993): $V=10.21$ and $B - V=+0.74$), whose constancy during the run was confirmed using a check star GSC 1117.2131 (star *d* in Howell et al. (1993)). Since EF Peg is a close double (separation 5.3") with a star (star *w* in Howell et al. (1993)), the resultant aperture photometry is a combined magnitude with this companion. The V -magnitude of the companion was measured as $V=12.71$ on a CCD from taken on 1992 May 5, when EF Peg was back in quiescence. As reported in Howell et al. (1993), EF Peg was brighter than this companion during the time of our observation. No variability has been yet reported for this companion star. Barycentric corrections to observed times were applied before the following analysis.

3 Results

3.1 Outburst light curve

The overall light curve of the superoutburst, drawn from the present observation, is presented in 1. The contribution from the nearby companion has been subtracted. The figure corresponds to the early part of Fig. 2 in Howell et al. (1993). The fading was slower (0.08 mag d^{-1}) for the first three nights, but became more rapid (0.14 mag d^{-1}) after October 20 ($\sim 5 \text{ d}$ after the detection of the outburst). The decline rate of 0.11 mag d^{-1} in Howell et al. (1993) apparently corresponds to an average of these values. The light curve of the outburst is a quite typical one for an SU UMa-type superoutburst.

3.2 Superhump period and profile

As later shown in 6 and also presented by Howell et al. (1993), EF Peg showed strong superhumps during the 1991 October superoutburst. In order to determine the superhump period, we applied the Phase Dispersion Minimization (PDM) method (Stellingwerf, 1978) to all the data, after removing the linear trends of decline, and after prewhitening for slow variations with frequencies smaller than 2 d^{-1} . The resultant theta diagram is shown in figure 2. The signal at the frequency 11.488 d^{-1} corresponds to the mean superhump period (P_{SH}) of $0.08705(1) \text{ d}$. Figure 3 shows the averaged profile of superhumps. The phase zero is taken as BJD

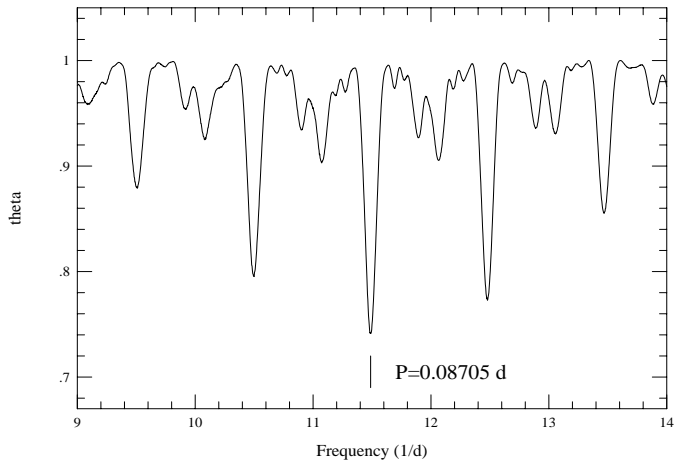


Figure 2: Period analysis of superhumps in EF Peg. The Phase Dispersion Minimization (PDM) method (Stellingwerf, 1978) was used, after removing the linear trends of decline, and after prewhitening for slow variations with frequencies smaller than 2 d^{-1} . The signal at the frequency 11.488 d^{-1} corresponds to the mean superhump period of $0.08705(1) \text{ d}$.

(Barycentric Julian Date) 2448547.953 (1991 October 18.453 UT). The averaged profile of superhumps is a typical one for an SU UMa-type dwarf nova: a steeper rise and a slower decline (Kato et al., 1998).

Figure 4 shows nightly averaged profiles of superhumps. The amplitude of superhumps reached a maximum on October 20 ($\sim 5 \text{ d}$ after the detection of the outburst), and slowly decayed after that. The phase zero is defined as BJD 2448547.953. The shifts of superhump maxima from the zero phases represent the $O - C$ variation described in Section 3.3.

3.3 Superhump period change

In order to determine the superhump period change, we extracted by eye superhump maxima times from our data and from the published light curves by Howell et al. (1993). The averaged times of a few to several points close to the maximum were used as representatives of the maxima times. The errors of maxima times are usually less than $\sim 0.003 \text{ d}$. The maxima times from the light curves in Howell et al. (1993) have been corrected to the common BJD system. The resultant superhump maxima are given in table 2. The values are given to 0.0001 d for the Ouda data in order to avoid the loss of significant digits in the later analysis. The cycle count (E) is defined as the cycle number since BJD 2448547.952 (1991 October 18.452 UT). A linear regression to the observed superhump times, gives the following ephemeris.

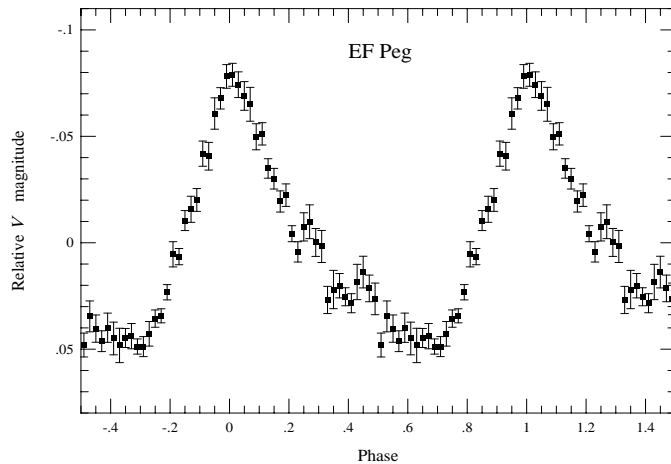


Figure 3: Phase-averaged light curve of EF Peg superhumps.

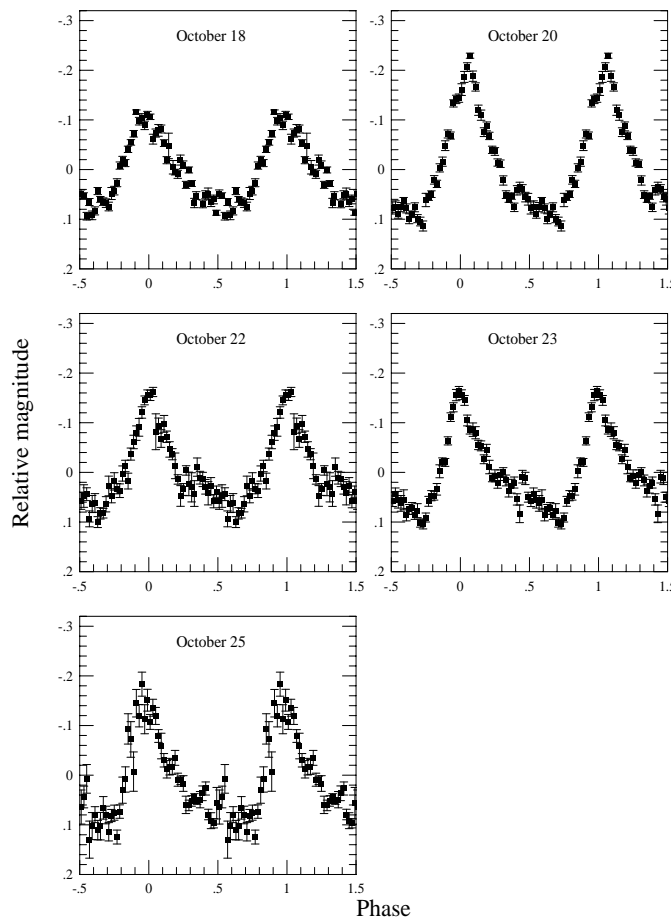


Figure 4: Evolution of EF Peg superhumps.

Table 2: Times of superhump maxima

E^*	BJD-2400000	$O - C^\dagger$	Ref. [‡]
0	48547.9517	-0.0119	1
1	48548.0388	-0.0117	1
9	48548.750	0.005	2
23	48549.9604	-0.0012	1
46	48551.9590	-0.0006	1
47	48552.0439	-0.0025	1
52	48552.481	0.000	2
53	48552.568	0.000	2
57	48552.9125	-0.0026	1
58	48553.0014	-0.0006	1
59	48553.0899	0.0011	1
64	48553.543	0.020	2
80	48554.9177	0.0046	1
81	48555.0018	0.0019	1
82	48555.0888	0.0020	1
87	48555.522	0.001	2
88	48555.612	0.004	2
98	48556.480	0.003	2
99	48556.569	0.005	2
110	48557.521	0.002	2
111	48557.607	0.001	2
122	48558.573	0.012	2
133	48559.512	-0.005	2
145	48560.553	-0.007	2
156	48561.506	-0.009	2
157	48561.591	-0.011	2

*Cycle count since BJD 2448547.952.

[†] $O - C$ calculated against equation 1.

[‡]1: this paper,

2: Howell et al. (1993).

$$\text{BJD}_{\text{max}} = 2448547.9636 + 0.086868E. \quad (1)$$

Figure 5 shows the $O - C$'s against the linear regression, equation 1. The diagram clearly shows the decrease of the superhump period, which was not apparent in the analysis by Howell et al. (1993), who used nightly determined superhump periods, rather than the $O - C$ analysis. After rejecting maxima times ($E=9, 64, 122$) having $|O - C| > 0.01\text{d}$ from a quadratic fit using all observed times, we obtained the following final quadratic equation.

$$\text{BJD}_{\text{max}} = 2448547.9512(20) + 0.087240(52)E - 2.21(31) \times 10^{-6}E^2. \quad (2)$$

The quadratic term corresponds to $\dot{P} = -4.4 \pm 0.6 \times 10^{-6} \text{ d cycle}^{-1}$, or $\dot{P}/P = -5.1(0.7) \times 10^{-5}$.

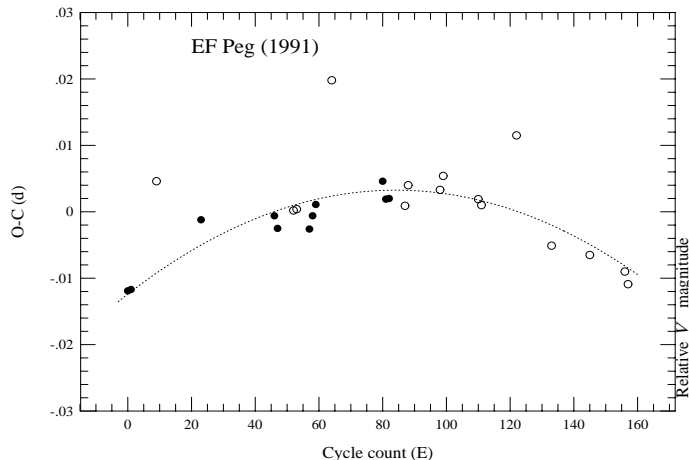


Figure 5: $O - C$ diagram of superhump maxima. Filled and open circles correspond to maxima times by this work and by Howell et al. (1993), respectively. The parabolic fit corresponds to equation 2.

4 Super-quasi-periodic oscillations

The most prominent feature detected during this outburst is large-amplitude super-quasi-periodic oscillations (super-QPOs: cf. Kato et al. (1992)), seen on 1991 October 18, ~ 2 d before the full growth of superhumps. These QPOs had disappeared on October 20. Figure 6 shows the light curve on 1991 October 18. Two superhump maxima separated by 0.087 d are clearly seen. The errors of individual measurements are ~ 0.01 mag. The detailed structure in the light curve therefore reflects the real variation of EF Peg. Rapid fluctuations superimposed on superhumps represent super-QPOs.

In order to more clearly show the structure of super-QPOs, we have subtracted superhumps from this light curve, by using a Fourier decomposition of the superhump profile up to the fourth harmonics. The resultant residual light curve is shown in figure 7.

Figure 8 shows the overall power spectrum of the prewhitened data (figure 7) on October 18. The strongest signal (210 d^{-1}) corresponds to the dominant frequency of super-QPOs. The presence of considerable power at lower frequencies indicates the quasi-periodic nature of the signal. Figure 9 shows the variation of the dominant QPO frequency within the October 18 run. The upper and lower panels show the power spectra of the first and second half of the October 18 run, respectively. The dominant frequencies are 81 d^{-1} ($P=18 \text{ m}$) and 213 d^{-1} ($P=6.8 \text{ m}$), respectively.

We determined the maxima times of super-QPOs by fitting a parabola to each super-QPOs (after remov-

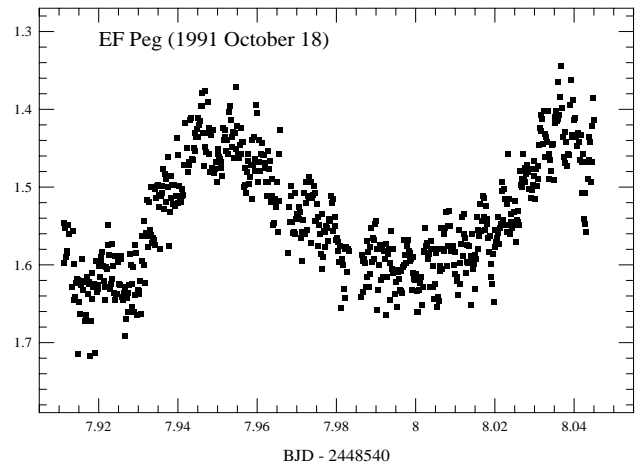


Figure 6: Light curve on 1991 October 18. Two superhump maxima separated by 0.087 d are clearly seen. Rapid fluctuations superimposed on superhumps represent super-QPOs.

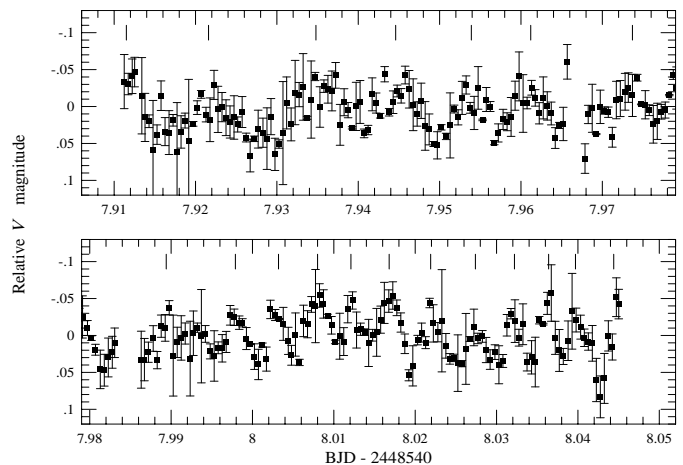


Figure 7: Super-QPOs, after subtracting the superhump variation from 6. The vertical ticks represent the maxima of super-QPOs listed in 3. The rapid decrease of the period of super-QPOs is clearly seen.

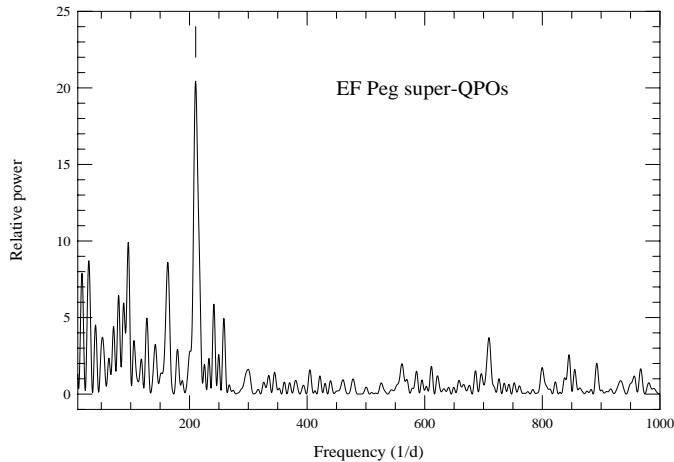


Figure 8: Power spectrum of super-QPOs. The strongest signal (210 d^{-1}) corresponds to the dominant frequency of super-QPOs. The presence of considerable power at lower frequencies indicates the quasi-periodic nature of the signal.

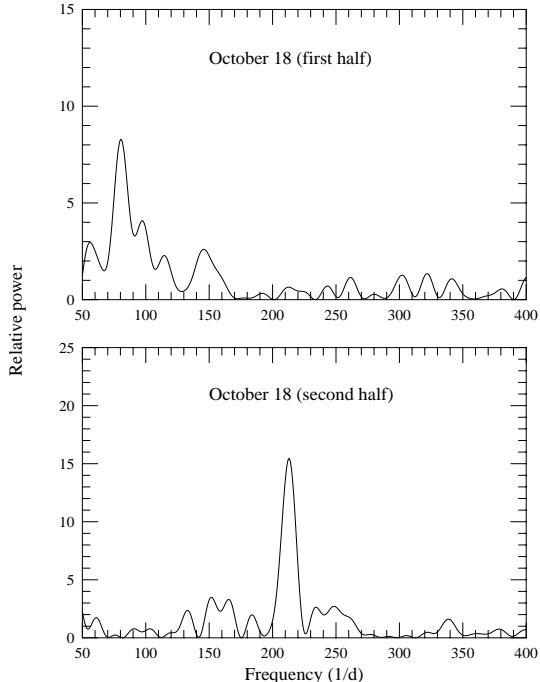


Figure 9: Variation of the QPO frequency. The upper and lower panels show the power spectra of the first and second half of the October 18 run, respectively. The dominant frequencies are 81 d^{-1} ($P=18 \text{ m}$) and 213 d^{-1} ($P=6.8 \text{ m}$), respectively.

Table 3: Times of maxima of super-QPOs

E^*	BJD [†]	$O - C^‡$
0	7.9115	-0.0130
1	7.9216	-0.0094
2	7.9348	-0.0026
3	7.9446	0.0007
4	7.9539	0.0036
5	7.9612	0.0044
7	7.9737	0.0040
9	7.9894	0.0068
10	7.9979	0.0088
11	8.0032	0.0077
12	8.0080	0.0060
13	8.0121	0.0037
14	8.0168	0.0019
15	8.0219	0.0006
16	8.0274	-0.0004
17	8.0322	-0.0020
18	8.0364	-0.0043
19	8.0397	-0.0074
20	8.0444	-0.0092

*Cycle count since BJD 2448547.9115

[†]BJD-2448540.

[‡] $O - C$ calculated against equation 3.

ing the superhump signal) around their maxima. The error of the estimates is typically 0.0002 d . The resultant times of maxima are listed in table 3. Although the observation was almost completely continuous, the maxima of $E=6, 8$ fell in short gaps of the observation.

A linear regression to the observed maxima gives the following equation.

$$\text{BJD}_{\text{max}} = 2448547.9245 + 0.006454E. \quad (3)$$

The variation of $O - C$'s (figure 10 and equation 3 indicates a large contribution of the quadratic (or higher) term. The following quadratic equation globally represents the overall $O - C$ variation, although there still exists small residual $O - C$'s to the quadratic equation.

$$\begin{aligned} \text{BJD}_{\text{max}} = & 2448547.9141(11) + 0.009988(25)E \\ & - 1.79(12) \times 10^{-4}E^2. \end{aligned} \quad (4)$$

The quadratic term corresponds to $\dot{P} = -2.6 \pm 0.2 \times 10^{-4} \text{ d cycle}^{-1}$. By adopting the mean period (0.00645 d) of super-QPOs from equation 3, the period change corresponds to a decay time-scale of $P/\dot{P} \sim 25$ cycles, or 0.16 d .

Figure 11 shows the averaged profile of super-QPOs. The phase zero was determined using maxima

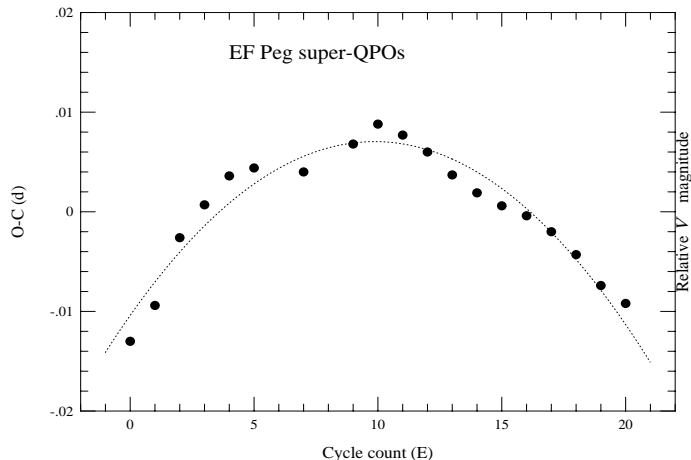


Figure 10: $O - C$ diagram of maxima times of super-QPOs, listed in table 3. The parabolic fit corresponds to equation 4.

epochs in table 3. The resultant averaged profile has a full amplitude of 0.05 mag.

5 Discussion

5.1 Superhump period change

As described in Section 3.3, EF Peg showed a decrease of the superhump period at a rate of $\dot{P} = -4.4 \pm 0.6 \times 10^{-6} \text{ d cycle}^{-1}$, or $\dot{P}/P = -5.1(0.7) \times 10^{-5}$. This negative period derivative has a typical value for long-period SU UMa-type dwarf novae (cf. Kato et al. (2001); Patterson et al. (1993); Kato et al. (1998)). However, the same EF Peg showed virtually zero period change during the 1997 superoutburst (Matsumoto et al., in preparation). While only a few SU UMa-type systems have been observed during different superoutbursts, all known systems showed relatively constant \dot{P} even in different superoutbursts (Kato et al., 2001). If such a large variation of \dot{P} in EF Peg is confirmed by future observations, EF Peg would be a unique system with regards to the stability of \dot{P} . Kato et al. (1998) proposed that positive \dot{P} in some short-period SU UMa-type systems may be a result of outward propagation of the eccentricity wave (cf. Lubow (1992); Baba et al. (2000)). The large variation of \dot{P} , proposed by the present observation of EF Peg, may reflect the different locations where tidal instability ignites.

5.2 Super-QPOs

As described in Section 4, EF Peg showed remarkable quasi-periodic oscillations (QPOs) during the earliest stage of the superoutburst, i.e. the growing stage of su-

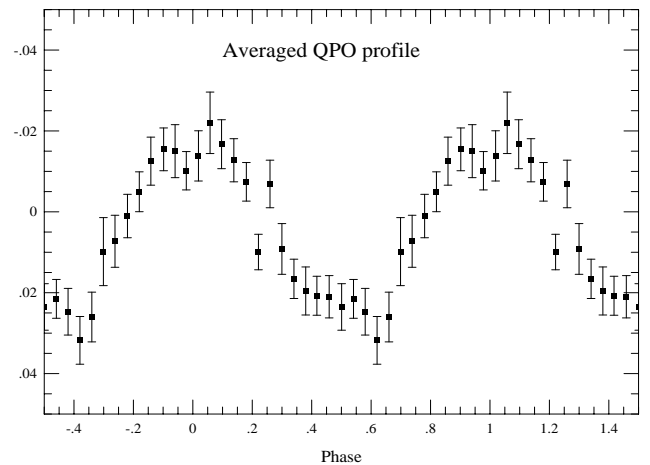


Figure 11: Averaged profile of the super-QPOs. The phase zero was determined using maxima epochs in table 3 (note that cycle lengths of individual QPOs are not constant). The resultant averaged profile has a full amplitude of 0.05 mag.

perhumps (October 18). These QPOs had disappeared when the amplitude of superhumps reached the maximum (October 20). As seen in 10, the maximum jump in the QPO phase was less than 0.002 d, indicating that the oscillations were essentially coherent during the entire observing run covering 20 QPO cycles, although a strong global variation of the period was present. Such a long coherence of oscillations is a signature of super-QPOs (Kato et al., 1992). Although the amplitudes of the present QPOs were smaller than that recorded in SW UMa during the 1992 superoutburst (Kato et al., 1992), they were larger than those of QPOs observed by Robinson et al. (1987) for the same star. The observed QPO profile and amplitude (figure 11) resemble those of the sinusoidal component of (Kato et al., 1992). From the transient appearance in the early stage of a superoutburst and the large amplitudes, we consider the present QPOs as a variety of super-QPOs. The same explanation in Kato et al. (1992) could apply to the present large-amplitude QPOs, except that the present QPOs incidentally lack the dip component.

The rapid decrease of the QPO period (figure 9, 10) is the unique characteristic of the present QPOs. Such a large variation of the QPO frequency within a short time (less than 3.2 hr) has never been observed in other QPOs of CVs. Furthermore, the period decrease occurred continuously (Section 4), rather than a sudden mode switch between different periods. The phenomenon is hard to explain, if these QPOs arise from oscillations of the accretion disk, or from the beat between the rotation of the magnetic white dwarf and the slowly rotating part of the accretion disk. Such a rapid

decrease of the QPO period can be more naturally understood if the rotating blob (cf. Kato et al. (1992)), which rapidly lost its angular momentum via the viscosity in a turbulent disk. If we assume a $1 M_{\odot}$ primary and nearly Keplerian orbits, a decrease of the period from 18 m to 6.8 m corresponds to a decrease of the radius of the orbit from $1.6 \cdot 10^{10}$ to $8.3 \cdot 10^9$ cm. This decrease in 3.2 hr corresponds to a radial velocity of $6.7 \cdot 10^5$ cm s $^{-1}$ (1/140 – 1/200 of the orbiting velocity), which seems to be a reasonable value for accretion during outburst.

5.3 Comparison with QPOs in XBs

Although such a rapid decrease of the QPO period is unique among CVs, there are a few known similar examples in oscillations (or large-amplitude QPOs) in some XBs. The best-known example is seen in the Rapid Burster (MXB 1730-335). The first indication of such oscillations during its type II bursts from the Rapid Burster was found with the GINGA satellite (Tawara et al., 1982). Dotani et al. (1990) systematically studied these oscillations, and found the evidence of strong period changes. The best example of the “naked-eye” visibility of large-amplitude oscillations and the rapid decrease of their periods can be found in Lubin et al. (1992b) [see also Lubin et al. 1991,1992a; for a recent observational review, see also Guerriero et al. (1999)].

The second example of similar oscillations was found in the bursting X-ray pulsar GRO J1744-28 (Zhang et al. (1996); Lewin et al. (1996)). The characteristics of the oscillations in GRO J1744-28 was studied in detail by Kommers et al. (1997). Although the nature of such oscillations are still poorly understood, several attempts have been made to understand these two unique objects. In the case of GRO J1744-28, Cannizzo (1996) considered an interplay between radial and vertical energy transport in the accretion disk, causing oscillations in the fraction of the gas pressure to the total pressure. Cannizzo (1996) showed that these oscillations eventually lead to a Lightman-Eardley instability (Lightman, Eardley, 1974), which Cannizzo (1996) considered to be the cause of Type II bursts. Cannizzo (1997) further showed that the characteristic QPO frequency can be reproduced by a selection of parameters. Abramowicz et al. (1995) suggested that low-frequency QPOs in some XBs (including those of the Rapid Burster) and black-hole candidates can be produced via dissipation of energy in the coronal region above the accretion disk. While these models were able to reproduce some parts of characteristics of QPOs (and bursts) observed in these systems, they have not yet succeeded in explaining a rapid decrease of QPO periods; the cause of this phenomenon is thus still an open question. These models for the Rapid Burster and GRO J1744-28 assume the strong radiation pressure near the

inner edge of the accretion disk. Since such a condition is hard to achieve in a CV disk, the mechanisms proposed for QPOs in XBs would not be directly applicable to the present QPOs in EF Peg. However, the existence of phenomenologically similar QPOs both in CVs and XBs may provide future insight for the fundamental understanding the underlying mechanisms.

Acknowledgments

The author is grateful to Dr. T. Takata and Mr. Y. Tomita for helping the observation. The author is also grateful to the VSOLJ and VSNET observers for supplying vital observations, and especially to Patrick Schmeer for promptly notifying us of the 1991 outburst detection.

References

- Abramowicz, M. A., Chen, X. & Taam, R. E. 1995, *ApJ*, 452, 379
- Baba, H., Kato, T., Nogami, D., Hirata, R., Matsumoto, K. & Sadakane, K. 2000, *PASJ*, 52, 429
- Blumenthal, G. R., Yang, L. T. & Lin, D. N. C. 1984, *ApJ*, 287, 774
- Cannizzo, J. K. 1996, *ApJ*, 466, L31
- Cannizzo, J. K. 1997, *ApJ*, 482, 178
- Collins, T. J. B., Helfer, H. L. & van Horn, H. M. 1998, *ApJ*, 508, L159
- Collins, T. J. B., Helfer, H. L. & van Horn, H. M. 2000a, *ApJ*, 534, 934
- Collins, T. J. B., Helfer, H. L. & van Horn, H. M. 2000b, *ApJ*, 534, 944
- Cox, J. P. 1981, *ApJ*, 247, 1070
- Dotani, T., Mitsuda, K., Inoue, H., Tanaka, Y., Kawai, N., Tawara, Y., Makishima, K., van Paradijs, J., Penninx, W., van der Klis, M., Tan, J. & Lewin, W. H. G. 1990, *ApJ*, 350, 395
- Esch, M. 1937, *Astron. Nachr.*, 264, 305
- Gessner, H. 1988, *Inf. Bull. Var. Stars*, 3209
- Guerriero, R., Fox, D. W., Kommers, J., Lewin, W. H. G., Rutledge, R., Moore, C. B., Morgan, E., van Paradijs, J., van der Klis, M., Bildsten, L. & Dotani, T. 1999, *MNRAS*, 307, 179
- Hildebrand, R. H., Spillar, E. J., Middleditch, J., Patterson, J. J. & Stiening, R. F. 1980, *ApJ*, 238, L145

- Hirose, M. & Osaki, Y. 1990, PASJ, 42, 135
- Hoffmeister, C. 1935, *Astron. Nachr.*, 255, 407
- Howell, S. B., Schmidt, R., Deyoung, J. A., Fried, R., Schmeer, P. & Gritz, L. 1993, PASP, 105, 579
- Kato, S. 1978, MNRAS, 185, 629
- Kato, T., Hirata, R. & Mineshige, S. 1992, PASJ, 44, L215
- Kato, T., Nogami, D., Baba, H. & Matsumoto, K. 1998, ASP Conf. Ser. 137, *Wild Stars in the Old West*, ed. S. Howell, E. Kuulkers & C. Woodward (San Francisco: ASP), p. 9
- Kato, T., Sekine, Y. & Hirata, R. 2001, PASJ, in press
- Kato, T. & Takata, T. 1991, IAU Circ., 5371
- Kommers, J. M., Fox, D. W., Lewin, W. H. G., Rutledge, R. E., van Paradijs, J. & Kouveliotou, C. 1997, ApJ, 482, L53
- Lewin, W. H. G., Rutledge, R. E., Kommers, J. M., van Paradijs, J. & Kouveliotou, C. 1996, ApJ, 462, L39
- Lightman, A. P. & Eardley, D. M. 1974, ApJ, 187, L1
- Lubin, L. M., Lewin, W. H. G., Dotani, T., Oosterbroek, T., Mitsuda, K., Magnier, E., van Paradijs, J. & van der Klis, M. 1992a, MNRAS, 256, 624
- Lubin, L. M., Lewin, W. H. G., Rutledge, R. E., van Paradijs, J., van der Klis, M. & Stella, L. 1992b, MNRAS, 258, 759
- Lubin, L. M., Lewin, W. H. G., Tan, J., Stella, L. & van Paradijs, J. 1991, MNRAS, 249, 300
- Lubow, S. H. 1992, ApJ, 401, 317
- Ohtani, H., Uesugi, A., Tomita, Y., Yoshida, M., Kosugi, G., Noumaru, J., Araya, S. & Ohta, K. 1992, *Memoirs of the Faculty of Science, Kyoto University, Series A of Physics, Astrophysics, Geophysics and Chemistry*, 38, 167
- Okuda, T. & Mineshige, S. 1991, MNRAS, 249, 684
- Okuda, T., Ono, K., Tabata, M. & Mineshige, S. 1992, MNRAS, 254, 427
- Papaloizou, J. & Pringle, J. E. 1978, MNRAS, 182, 423
- Patterson, J. 1979, ApJ, 234, 978
- Patterson, J. 1981, ApJS, 45, 517
- Patterson, J., Bond, H. E., Grauer, A. D., Shafter, A. W. & Mattei, J. A. 1993, PASP, 105, 69
- Politano, M., Howell, S. B. & Rappaport, S. 1998, ASP Conf. Ser. 137, *Wild Stars in the Old West*, ed. S. Howell, E. Kuulkers & C. Woodward (San Francisco: ASP), p. 207
- Robinson, E. L. 1973, ApJ, 183, 193
- Robinson, E. L., Shafter, A. W., Hill, J. A., Wood, M. A. & Mattei, J. A. 1987, ApJ, 313, 772
- Sandig, H. U. 1950, *Astron. Nachr.*, 279, 89
- Schmeer, P. & Poyner, G. 1991, IAU Circ., 5369
- Stellingwerf, R. F. 1978, ApJ, 224, 953
- Szkody, P. 1976, ApJ, 207, 190
- Tawara, Y., Hayakawa, S., Hunieda, H., Makino, F. & Nagase, F. 1982, *Nature*, 299, 38
- Tsesevich, V. P., Goranskij, V. P., Samus', N. N. & Shugarov, S. Y. 1979, *Astron. Tsirk.*, 1043, 3
- van der Klis, M. 1989, ARA&A, 27, 517
- van der Klis, M. 1999, in *Pulsar Timing, General Relativity and the Internal Structure of Neutron Stars*, ed. Z. Arzoumanian, F. Van der Hooft & E. P. J. van den Heuvel (Koninklijke Nederlandse Akademie van Wetenschappen, Amsterdam), p. 259
- van der Klis, M. 2000, ARA&A, 38, 717
- van Horn, H. M. & Wesemael, F. W. D. E. 1980, ApJ, 235, L143
- Warner, B. 1995a, *Cataclysmic Variable Stars* (Cambridge University Press, Cambridge)
- Warner, B. 1995b, Ap&SS, 226, 187
- Whitehurst, R. 1988, MNRAS, 232, 35
- Yamasaki, T., Kato, S. & Mineshige, S. 1995, PASJ, 47, 59
- Zhang, W., Morgan, E. H., Jahoda, K., Swank, J. H., Strohmayer, T. E., Jernigan, G. & Klein, R. I. 1996, ApJ, 469, L29